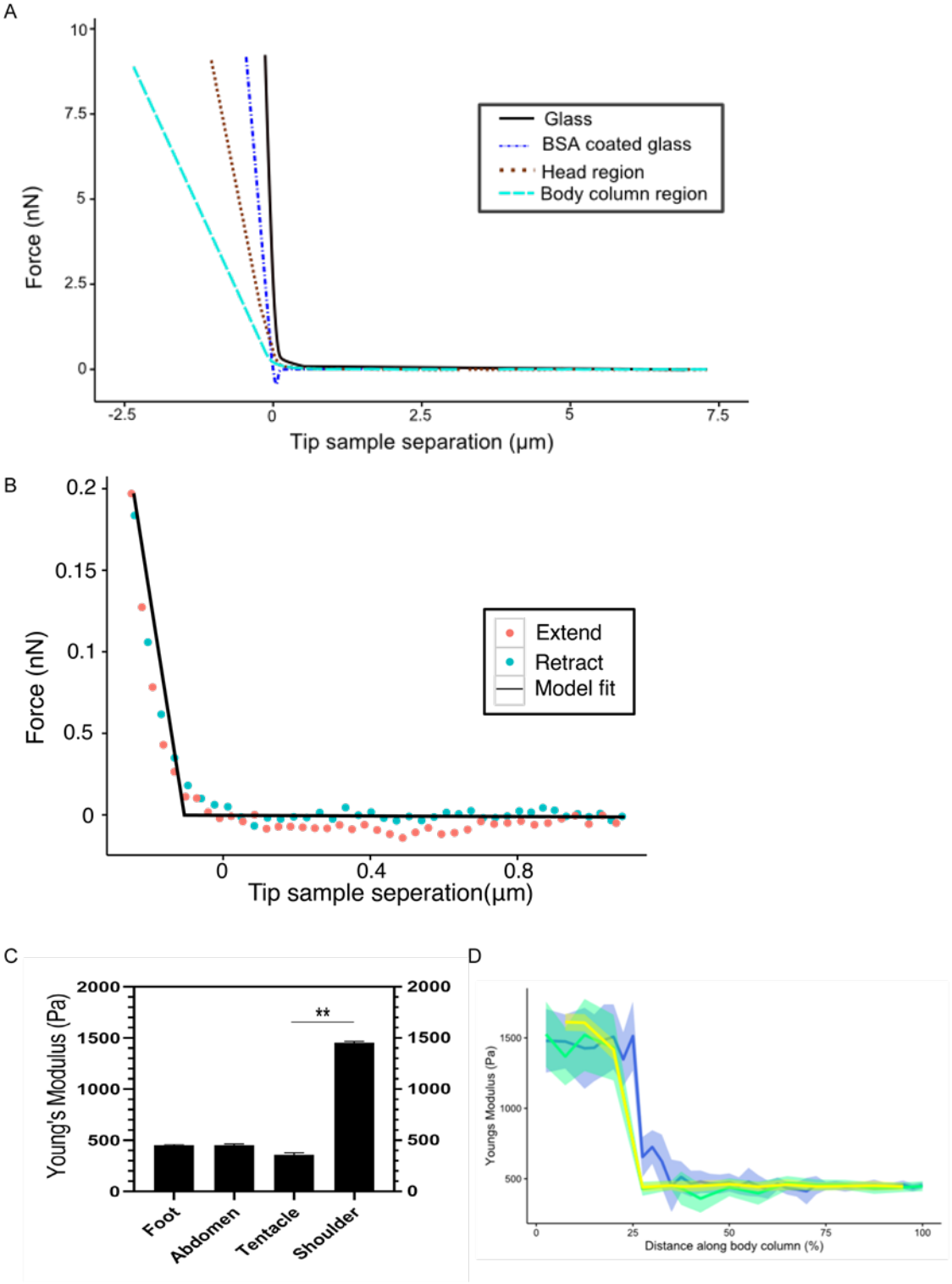

Figure S1. The variation in Young's Modulus is species independent.

A. The raw data of glass-glass, BSA coated coverslip -glass and *Hydra* tissue-glass contacts. The measurements clearly demonstrate that stiffness of the *Hydra* tissue is measured accurately.

B. The Hertz model works for non-adhesive elastic contacts. The plot shows approach and retract curve on *Hydra* tissue. The approach and retract curves show no hysteresis indicating no adhesion and the tissue has been elastically deformed. The Hertz model works for non-adhesive elastic contacts. The plot shows approach and retract curve on *Hydra* tissue. The approach and retract curves show no hysteresis indicating no adhesion and the tissue has been elastically deformed.

C. Measurement of Young's modulus over different parts of *Hydra* including the body column. The tentacles have nearly the same stiffness as body column except in the shoulder region. The shoulder region is three times stiffer.

D. Three biological replicates of *Hydra* (AFM measurements collected at 100 μm intervals shown in different colors) depict the change in Young's modulus in the same region of the body column. The ribbon shows the standard deviation of each individual experiment along the line signifying the average.

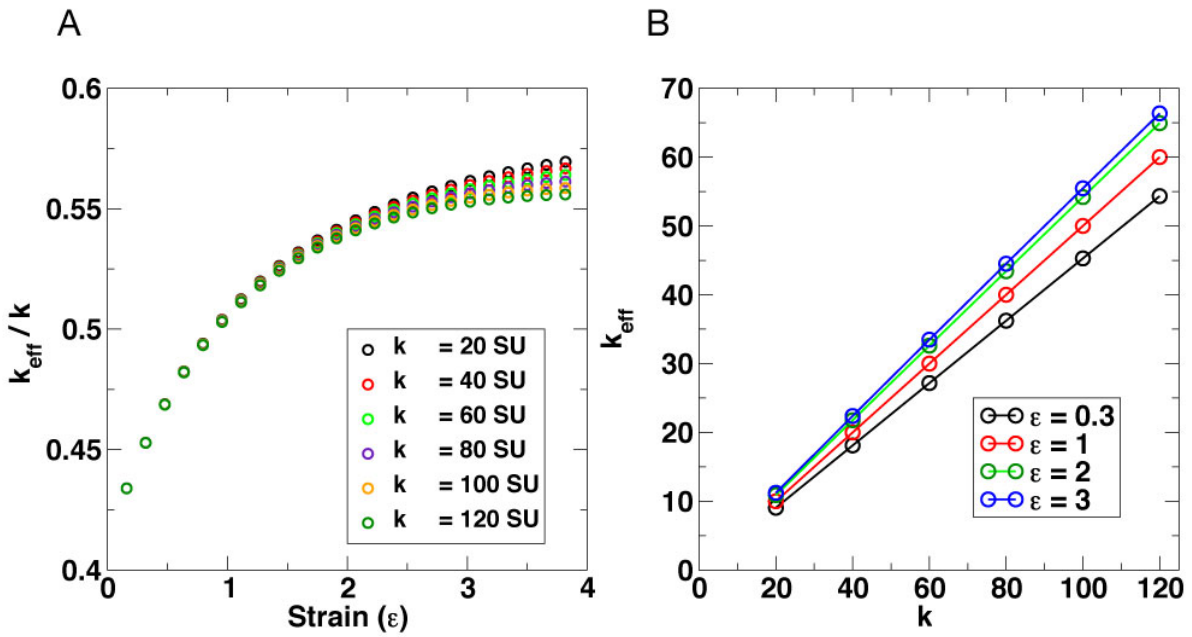

Figure S2. Modeling *Hydra* body column to represent various steps involved in the somersault movement.

A. The effective spring constant changes with increasing strain for lower values of ε because the diagonal springs contribute nonlinearly to the axial force but saturates at larger values of deformation. The plot shows the effective stiffness $k_{eff,}$ normalized by k - the spring constant of individual springs, versus the strain ε,. The k_{eff} is calculated by dividing F_{axial}, the extensional force applied along the axis, by the extension (L_0 -L) – where L_0 and L are neutral and stretched length of cylinder, respectively. For very high strains of ε = 3 and more. The saturation occurs because the angle between the diagonal springs (shown in Figure 4) and the parallel springs becomes very small for large strains, resulting in them being almost parallel to the axis and contributing equivalently to the effective spring constant as other springs.

B. k_{eff} can be conveniently tuned by choice of k as k_{eff} varies linearly with k for each value of ε. We have described the *Hydra* body column as cylinder of uniform cross-section made up of mass-points as shown in Figure 4A. This helps in tuning the stiffness of the body column as seen in AFM experiments (α = 3).

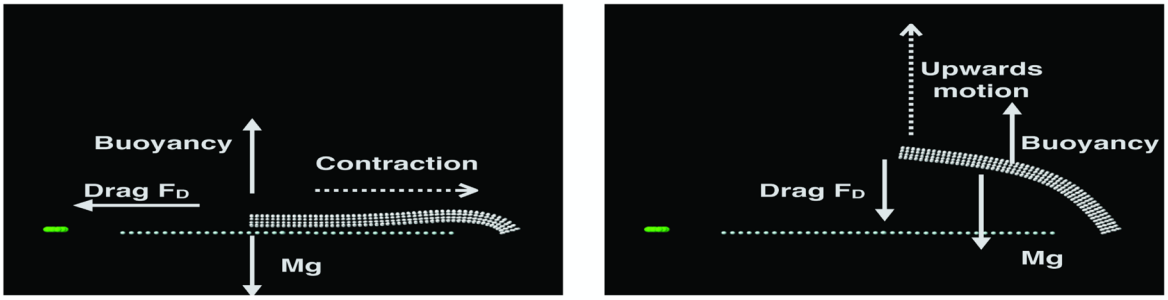

Figure S3. Various forces acting on *Hydra* body column at different stages. The viscous drag force acting on ith bead is equal to $F_D = - \Gamma i\ vi$. The total friction constant $\Gamma = \sum \Gamma i$. The summation is over 500 beads. Assuming most of the downward gravitational force is balanced by buoyancy; each mass point experiences only a small fraction of net downward force due to gravity. We take density difference between *Hydra* and water to be about 5% or higher as seen in the experiments.

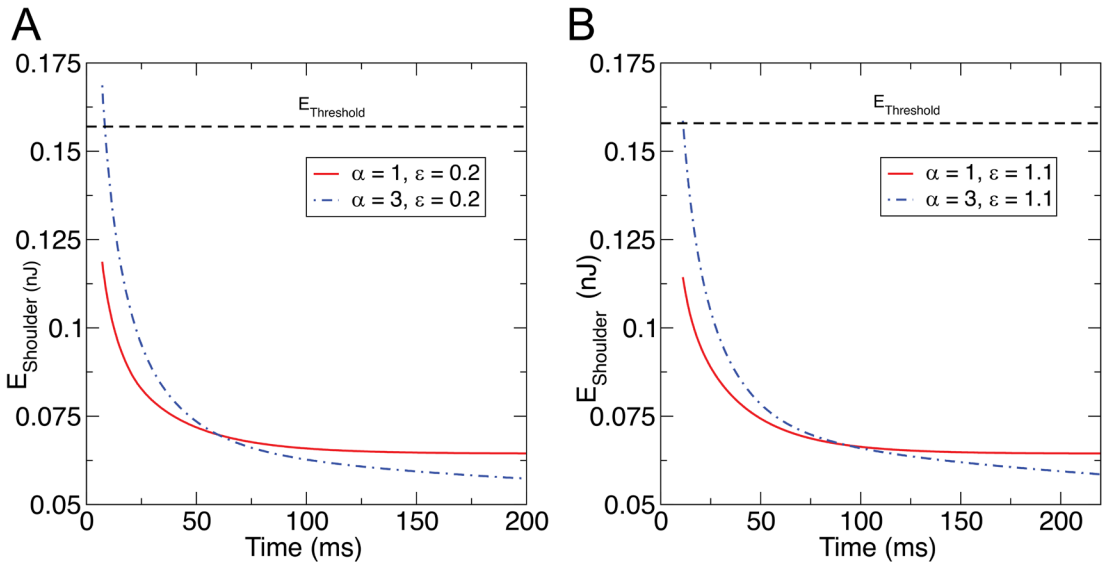

Figure S4. The plots of potential energies in shoulder versus time. **A.** The energy in shoulder around 10 ms after release is more for α =3 and below threshold for α =1. for strain of 0.2. The dashed line shows the energy threshold required to stand up- side down as described in Figure 3*A* and the appendix A1.

B. The plots of energy in the shoulder versus time for strain of 1.1. We show that for strains as different as 0.2 and 1.1, the energy in the shoulder is above threshold for α =3 than α =1. The initial energies in both these cases were as different as 2.4 nJ and 42 nJ.

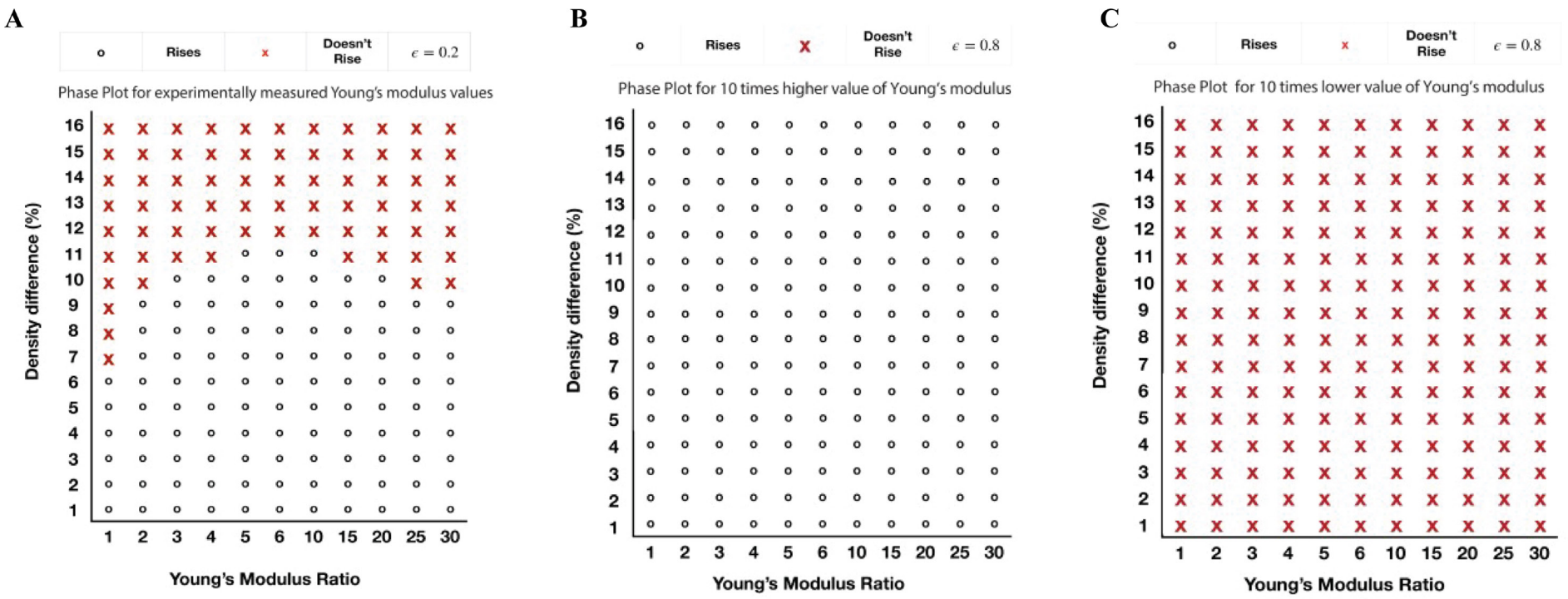

Figure S5: Phase diagrams for various mechanical parameters of *Hydra*.

Journal of Experimental Biology: doi:10.1242/jeb.232702: Supplementary information

Figure S5. Phase diagrams for various mechanical parameters of *Hydra*.

A. The phase diagram for strain ε= 0.2. Note that the overall energy in the stretch is reduced due to smaller strains. The dissipated energy while the body column is contracting is much less too. Hence, the tissue stiffness variation is not very critical for density difference of 6 percent and below. Albeit the *Hydra* with larger variation in tissue stiffness characterized by larger α is able to lift body columns with density difference with respect to water of up to 9-10 percent.

B. Phase plots for stiffness values which are 10 times larger than those observed in AFM experiments. The criticality observed with stiffness values in the range seen in AFM experiments is absent. The variation in tissue stiffness is not important. However, it should be noted that the energies involved in stretching and bending are too high and actual Hydra may not have so much energy if the body column is 10 times stiffer.

C. If the Young's modulus is 10 times lower than those observed in AFM experiments, the criticality is not seen with respect to variation in tissue stiffness. *Hydra* is not able to rise up. Such a labile *Hydra* polyp will be able stretch itself out easily but will not have enough energy transferred to shoulder to lift itself.

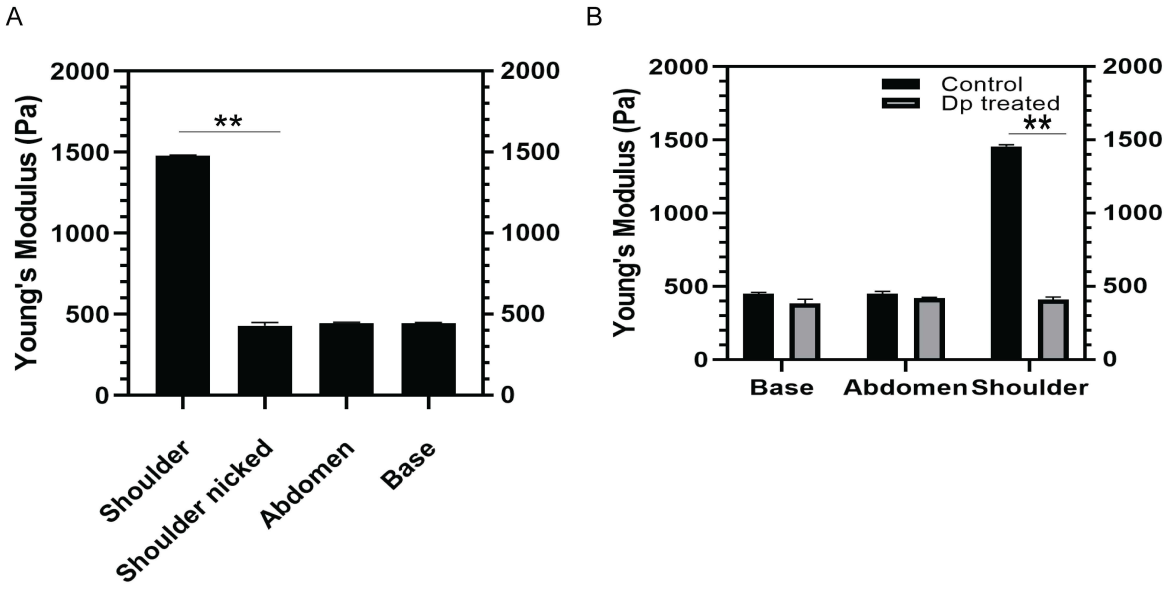

Figure S6. Measurement of Young's modulus after disruption of extracellular matrix.

A. The shoulder region of *Hydra* was nicked such that the polyp was cut halfway on one side (until the center of the body cavity) to disrupt the stiffness in this region. The polyp was allowed to heal for 12 hours after which AFM measurements were performed. The graph represents Young's Modulus (Pa) of three distinct regions of the body column after amputation in 3 biological replicates. Error bars show the standard error of mean between three biological replicates; significance value calculated by the student t test.

B. Young's modulus for *Hydra* polyps treated with the lysyl oxidase inhibitor Dipyridyl (solid black) shows the loss of the differential in Young's modulus between the shoulder and the rest of the body column as compared to the control (grey). The experiment is performed in three biological replicates with error bars showing the standard error of mean of the replicates, significance values calculated using the Student's t test. The Young's modulus is represented as calculated from hertz fit for the force curves.

Table S1

Click here to Download Table S1

Table S2

Click here to Download Table S2

Table S3

Click here to Download Table S3

Table S4

Click here to Download Table S4

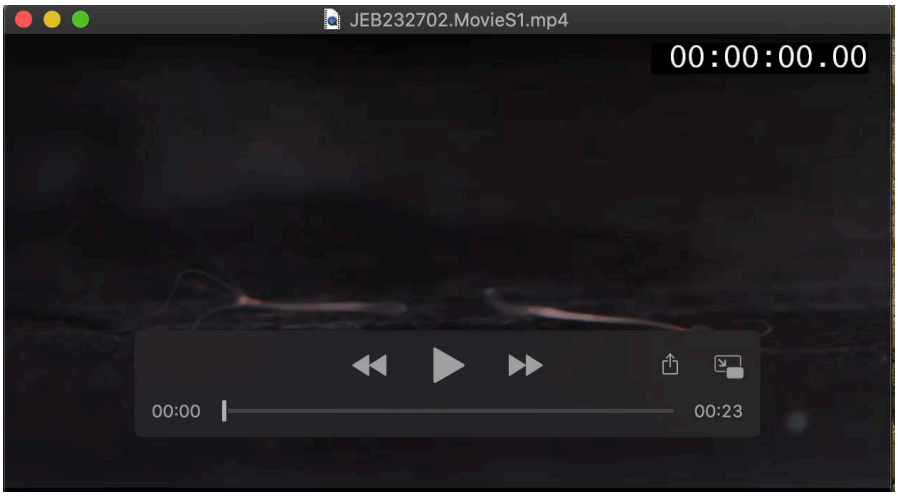

Movie 1. *Hydra* Somersault. This movie shows a typical *Hydra* polyp (on the right) performing the first half of the somersault i.e. turning upside down from a horizontal position. The *Hydra* on the left is resting horizontally on the substrate.

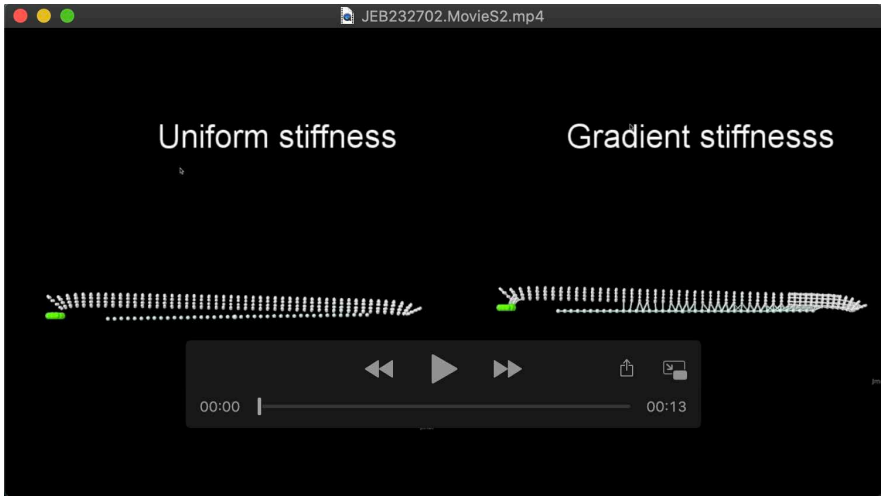

Movie 2. Hydra-model simulations show that the stiffness gradient is crucial for *Hydra* to somersault. This movie shows a comparison of two hydra-model simulations of with and without stiffness gradient.

Movie 3. Physical disruption of tissue stiffness in the shoulder region disables *Hydra* from somersaulting. This movie shows how disruption of local shoulder tissue stiffness by physical means (lesioning through a partial cut) can disable *Hydra* from performing somersault and not upon stiffness disruption in body column.

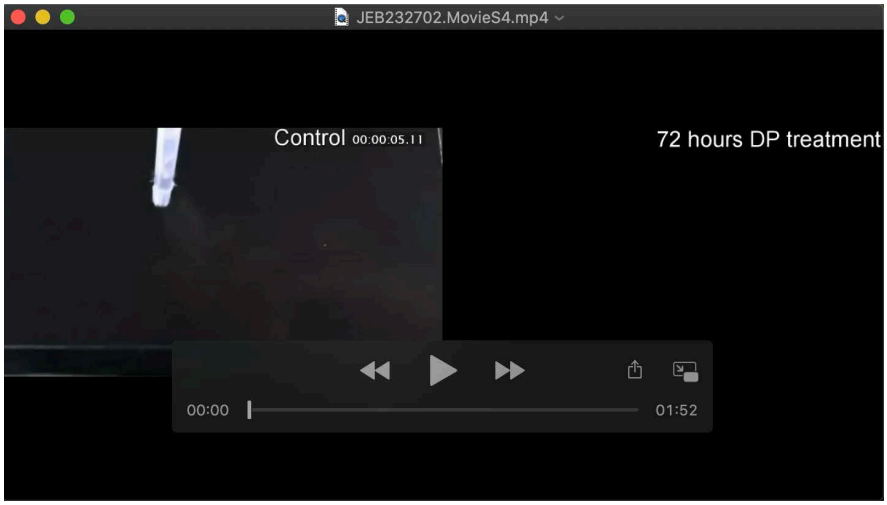

Movie 4. Chemical disruption of global tissue stiffness completely abrogates the capability of *Hydra* to somersault. This movie shows how disruption of global tissue stiffness by treatment with Dipyridyl (Dp) for 72 hrs of can completely disable *Hydra* from performing a somersault.

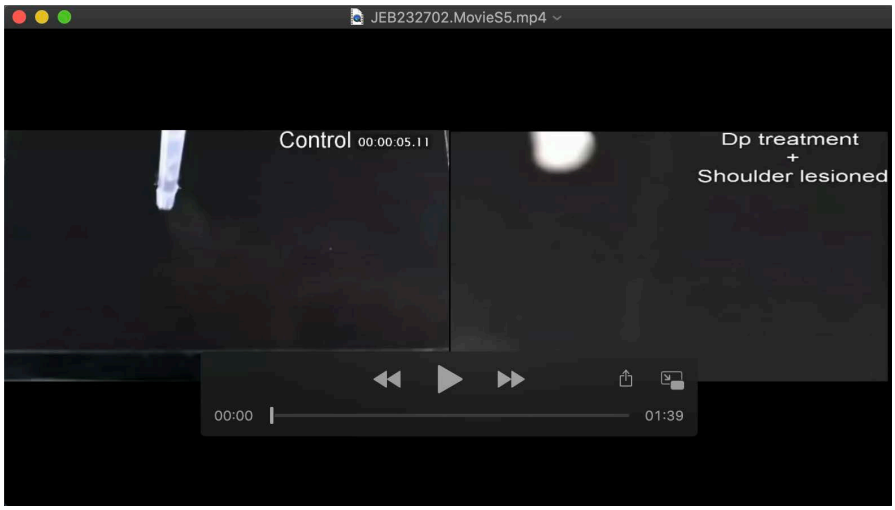

Movie 5. Chemical disruption of tissue stiffness in the shoulder region disables *Hydra* from somersaulting. This movie shows how selective disruption of collagen fibrils at the shoulder region by lesioning and letting the tissue regenerate in the presence of Dipyridyl can completely disable *Hydra* from performing a somersault.

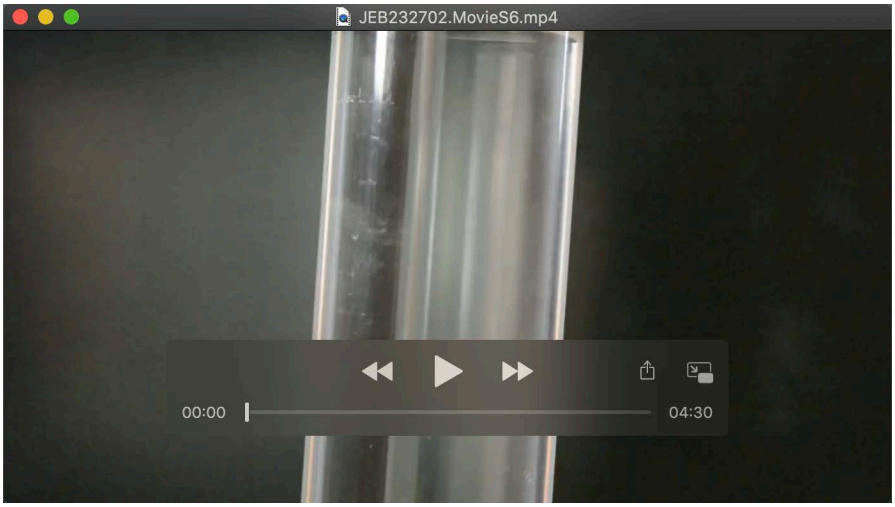

Movie 6. The measurement of *Hydra* density using its free fall in water: This movie shows Hydra after its tentacles removed and made to fall in the water column. The measurement of terminal velocity allows for the estimate of density.